

P. Vijay^{1*}, K.V. Brahma Raju², K. Ramji³, S. Kamaluddin⁴

¹ Raghu Institute of Technology, Visakhapatnam, India

² SRKR Engineering College, Bhimavaram, India

³ Andhra University, Visakhapatnam, India

⁴ Jamia Institute of Engineering and Management Studies Akkalkuwa, Maharashtra, India

* Corresponding author. E-mail: vijaypendhota86@gmail.com

Received (Otrzymano) 24.09.2021

EFFECT OF TUNGSTEN CARBIDE ON Al6061/SiC HYBRID METAL MATRIX COMPOSITES

Aluminium matrix composites (AMC) are mostly preferred for their high specific strength, high ductility, corrosion resistance and creep resistance. Various experimental investigations are conducted in the field of AMCs, which are widely applicable in several fields like aerospace (especially aircraft structures and fittings), marine fittings, automotive industries (connecting rods, pistons, brake rotors, and engine blocks), etc. The current work presents the effect of a tungsten carbide (WC) reinforced Al6061/SiC hybrid composites. In this study, the WC particle (3–5 µm) content is varied from 0 to 6 wt.% in steps of 2 wt.%, while keeping the SiC particle (63 µm) content of 5 wt.% constant. The stir casting method was used to prepare these composites and the behaviour of the composites was studied to ascertain their mechanical and corrosion properties. From the obtained results, it was observed that the ultimate tensile strength, hardness, and corrosion resistance of the composites are enhanced by increasing the content of WC, whereas the wear loss (microns) decreased as the WC was increased up to 4 wt.%; later it increased drastically at 6 wt.% WC. The corrosion results reveal that the corrosion rate of the composites is lower than that of the monolithic alloy. SEM examination of the tensile fracture surface shows that there is a formation of larger shear lips in the base alloy and the composite with 5 wt.% SiC; however, they are reduced gradually by the additions of WC to the composite. The microstructure of the corroded surfaces reveals that the pit density was reduced for the composite with 6 wt.% WC compared to the other composites.

Keywords: Al 6061, SiC, WC, stir casting, tensile strength, wear, corrosion

INTRODUCTION

In recent decades, AMCs have proved to be a good choice for engineering materials. AMCs have been making their mark particularly in the automobile industry to replace the components of heavy weight parts like pistons, cylinder liners, gears, brake drums, suspension components, connecting rods, valves, cylinder block drive shafts, etc. Significant work has been done recently on aluminium metal matrices reinforced with different ceramic materials like SiC, TiB₂, Al₂O₃, B₄C, WC, fly ash, etc. AlSi₇Mg₂ reinforced with SiC increases the tensile strength of the composite up to 10 wt.% SiC and decreases with a further increase of the particulate up to 15 wt.% due to de-bonding between the base alloy and the reinforcing particles at their interface. In the study of the microstructure, it was observed that clusters and porosities formed and the dispersion of the SiC particles is non-homogeneous [1, 2]. An aluminium metal matrix reinforced with WC slowly transforms from a ductile to a brittle nature by increasing the wt.% of WC. Reinforcing composites with WC up to 8 wt.% enhances the strength but it is reduced at 10 wt.% WC due to clustering of the WC particles [3]. Arivukkarasan et al. [4] illustrate that Al LM4 reinforced with 0, 5, 10, 15 wt.% WC improves

the tensile strength, hardness and wear properties of the composite by increasing the wt.% of WC and is the highest at the highest reinforcement. Al 6061 reinforced with WC 0–4 wt.% in increments of 1 wt.% reveals that the tensile strength and hardness of the composite increase by raising the WC content up to 3 wt.%, and a further increment in WC shows a decline in all the properties due to poor bonding between the base alloy and filler particles. It was also observed that the wear resistance was enhanced up to 3 wt.% WC, while beyond that it falls owing to the lower hardness of the composite [5]. The microstructure of Al6061/SiC/WC hybrid composites reveals that dissimilar reinforced particles are uniformly distributed and at some places, small clusters are detected, whereas in the SEM and XRD analysis it was observed that Mg₂Si formed as a consequence of an interfacial reaction between Al6061 and the reinforcements. In addition, the presence of undissolved Al₆ of the matrix enhances the mechanical properties [6]. AMCs reinforced with SiC/ B₄C show that the tensile strength, bending strength, and hardness increased thanks to the addition of reinforcing particulates, but the impact strength of the composite decreases as the wt.% of particles increases, and

because of that a composite with a low SiC content absorbs more energy than that of a composite with a high wt.% of SiC [7]. An aluminium metal matrix reinforced with a constant SiC content (10% by weight) and varying TiB₂ contents from 0 to 5 wt.% in increments of 2.5 wt.% reveals that the mechanical properties like tensile strength and hardness of the composite decrease as the wt.% of TiB₂ increases due to clustering of the TiB₂ particles at its highest wt.% around the SiC particles, which leads to porosity. Moreover, the wear resistance of the composite is improved up to the addition of 2.5 wt.% TiB₂, whereas it decreases at 5 wt.% TiB₂ owing to the presence of porosity [8]. Hybrid composites with double synthetic ceramics exhibited better mechanical behaviour compared with hybrid composites using agro-industrial waste derivatives as one of the filler materials along with the synthetic ceramics. Agro-industrial wastes are considered as complementing reinforcements to synthetic particulates, which display better properties than that of unreinforced alloys and because of their low density, accessibility and eco-friendliness, agro-industrial waste is substituted for synthetic ceramics [9]. An Al alloy reinforced with 10 wt.% SiC (constant content) and bamboo leaf ash (BLA) of 0, 2, 3, 4 wt.% illustrates that the tensile strength, elongation and hardness of the composite drops with increasing BLA owing to the presence of silica, but the fracture toughness of the composite with SiC/BLA is higher than that of the composite with SiC alone [10]. An aluminium metal matrix reinforced with Al₂O₃, graphite and rice husk ash (RHA), reveals that the hardness dwindles by increasing RHA because of the existence of silica, which is softer than alumina and graphite, and additionally softens the composite. The tensile strength increases at a graphite content of 0.5 wt.% and RHA 50 wt.% compared to that of the composite without graphite, while the wear loss of the composite is reduced by the accumulation of graphite due to the formation of a dense lubricating film between the contact surfaces [11]. The behaviour of the composite material depends upon the size and amount of reinforcement particles; decreasing the size of the particles and raising the wt.% of Al₂O₃ in an Al/Al₂O₃ composite improves the mechanical properties like tensile strength and hardness, but the porosity of the composite increases because of the extended particle feeding time and the reduced size of the particle, the surface area interaction with air is increased. SEM analysis reveals that larger sized particles are distributed uniformly, whereas finer particles form clusters, porosity and particle isolation, owing to particle rejection by the solid-liquid interface, and are segregated to the inter-dendritic region formed by pre-solidified Al dendrites [12]. The effect of MoS₂ in the Al6061/Al₂O₃ hybrid composite reveals that the tensile strength is the highest at the smallest wt.% of MoS₂ and the hardness is the highest at a high wt.% of MoS₂, while the wear and friction resistance improve due to the presence of a rich mixed layer of MoS₂ that protects the surface contact [13].

Al 6061 reinforced with SiC/Al₂O₃ of 5÷10 wt.% in increments of 2.5 wt.% and a constant 5 wt.% content of fly ash exhibits enhanced ultimate tensile strength as the wt.% of the reinforcement increases and low strength was obtained by Al 6061/5 wt.% SiC/5 wt.% Al₂O₃/5 wt.% FA because of inadequate adhesive bonding between the matrix and particulate. In contrast, the hardness of the composite moderately increases at 5 and 10 wt.% reinforcement and drastically increases at 7.5 wt.% reinforcement, but there is no considerable change in the impact strength [14]. An aluminium 7075 reinforced with fly ash composite prepared by the pressure infiltration process examined for different properties illustrates that the hardness of the composite increases, at the same time the thermal expansion and wear resistance of the composite decline with the addition of fly ash [15].

The results obtained by squeeze casting technology of an AK12-fly ash composite are more beneficial than that of those obtained by the gravity casting method, but the pitting corrosion of the composite with fly ash is greater than that of the base alloy due to presence of a higher silicon content, in addition to defects such as pores [16]. Sun Zhiqiang et al. [17] reported in their study that an aluminium metal matrix reinforced with 9Si/Al-Cu-Mg reduces the wear to less than that of the base alloy and from micrographs it is apparent that the wear mechanism of the composite alters from abrasion at low loads to delaminating at high loads because of de-bonding between matrix and the reinforcing particles. In the experimental investigation of Al535/fly ash composites, it was observed that the particles are distributed non-uniformly as they form clusters at the dendrite boundaries of the aluminium, which leads to the build-up of adverse porosity and reduces the mechanical properties of the composite by augmenting the fly ash content [18].

The mechanical properties of Al6061/SiC/Gr hybrid composites were increased in comparison to those of the Al6061/SiC composite, but the density of the composite with single reinforcement is more than the hybrid composite resulting from the absence of graphite, while the morphology of the composite ensures there is no segregation of SiC particles and that they are uniformly distributed [19]. By increasing the stirrer speed and time, the reinforcing particles will distribute homogeneously and the composite will exhibit enhanced mechanical properties [20].

An experimental study of the mechanical properties of AMC reinforced with fly ash (FA) and aloe vera (AV) separately, reveals that AV is eco-friendly and uniformly distributed compared to the FA particles and AMC-AV displays better results than that of pure Al and AMC-FA [21]. The hardness of the Al 359/SiC composite is better than that of Al359/SiC/Gr because the presence of Gr softens the composite; nonetheless, the ultimate tensile strength and wear properties of Al359/SiC/Gr are higher than the Al359/SiC owing to the good bonding of the composite [22].

MATERIALS

In the present work, the Al6061 alloy, containing silicon and magnesium as the main elements (as shown in Table 1) was chosen for the matrix because of its high strength, high weldability, good corrosion resistance, high thermal conductivity, and good electrical conductivity, whereas SiC and WC were selected for the reinforcing particles 63 and 3–5 µm in size, respectively. The main cause for considering different particle sizes is that larger size particles help to attain a homogeneous mixture and smaller size particles enhance strength [1].

TABLE 1. Chemical composition of Al 6061 alloy

Composition	Mg	Si	Fe	Cu	Zn	Ti	Mn	Cr	Others	Al
[%]	0.8-1.2	0.4-0.8	0.7	0.15-0.4	0.25	0.15	0.15	0.04-0.35	0.05	Bal

Properties like hardness and wear can be enhanced by the addition of SiC particles; however, the toughness of the composite can be lower due to the presence of hard particles. Owing to its properties of high thermal conductivity and good thermal shock resistance, SiC can be applied in components subjected to high heat transfer. WC is one of the hardest ceramic materials with equivalent contents of tungsten and carbon atoms that can be used as reinforcing particles in AMCs to enhance properties like strength, hardness and wear resistance. The properties of the Al 6061 alloy, silicon carbide and tungsten carbide are shown in Table 2.

TABLE 2. Properties of Al 6061, SiC, and WC

Property	Al 6061	SiC	WC
Density [g/cm³]	2.70	3.21	15.6
Poisson's ratio	0.33	0.14	0.21
Young's modulus	68.9	410	600
Melting point [°C]	585	2730	2785-2830
Thermal conductivity [W/m·K]	151-202	120	100

METHODOLOGY

Al 6061 hybrid composites were prepared by the stir casting process (Fig. 1a). Initially, the aluminium 6061 alloy block of the calculated weight was put in a graphite crucible and liquefied in an electric furnace over 800°C. When the matrix reached its molten state, the calculated amounts of preheated SiC and WC particles were gradually added. The reinforcing particles were mixed with the molten matrix using a stirrer setup at the speed of 400 rpm up to 6 minutes as shown in Figure 1b. While stirring, magnesium up to 1 wt.% was added to the molten matrix to improve the wettability, and

1 wt.% degassing powder was also added to extract gases from the melt. After the stirring was completed, the mixed melt was poured into a preheated metallic die and formed the solidified composite presented in Figure 1c.

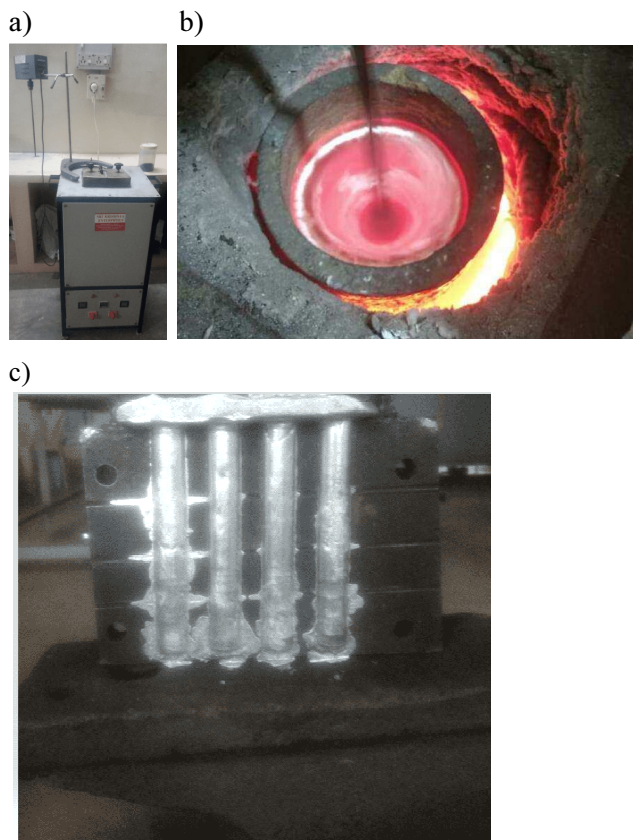


Fig. 1. Stir casting setup (a); molten state of composite (b), solidified composite in die (c)

Tensile testing was carried out on an INSTRON 8801 fatigue testing machine in which the ultimate strength was measured of test specimens under load subjected to controlled tension until failure. The specimens were prepared as per the ASTM E8 standard as shown in Figure 3 and the specifications of a standard specimen were tabulated as shown in Table 3. The specimen was placed between the upper and lower jaws of the testing machine, which hold the specimen tightly as shown in Figure 2b.

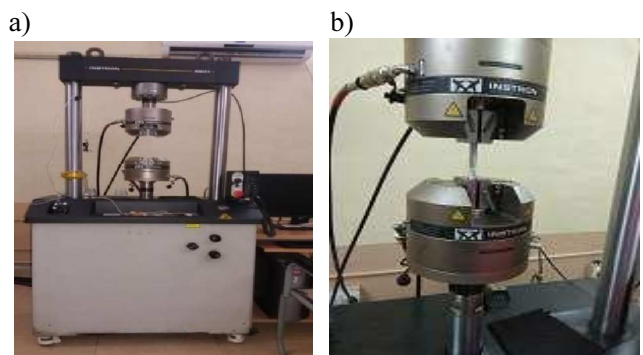


Fig. 2. Fatigue testing machine

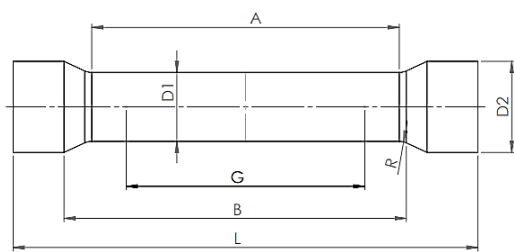


Fig. 3. Standard specimen for tensile test

Table 3. Specifications of tensile test specimen

Overall length L	122 mm
Distance between shoulders B	62 mm
Length of reduced parallel section A	56 mm
Gauge length G	50 mm
Fillet radius R	10
Diameter of reduced section $D1$	12.5 mm
Diameter of grip section $D2$	18 mm

SEM analysis of the tensile fractured surface was carried out at the Advanced Analytical Laboratory, Andhra University, on an INCA Penta FET x3 as shown in Figure 5, to study the surface morphology of the tensile fractured specimens at high magnification of 1000X, whose results are displayed in Figure 11a-e.

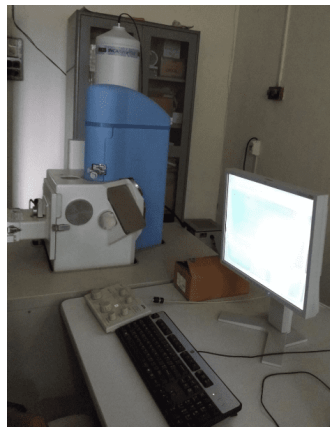


Fig. 5. INCA Penta FET x3

Hardness test

A hardness test was performed on specimens using a Vickers hardness tester (Fig. 6a) under the load of 0.25 kg. The test specimen should have a highly polished flat surface to easily notice the indentation mark made by the load applied on the specimen. These indentations marks can be observed by light microscope attached to the hardness tester. The indenter is a square-based pyramid with an angle 136° between the opposite faces of the pyramid and the indentation mark resembles a square cross-sectional area (Fig. 6b).

Thus, the diamond pyramid hardness number can be determined by Equation (1):

$$HV = 1.854 \frac{F}{D^2} \quad (1)$$

where F = applied force (load), $D = (d_1+d_2)/2$ (diagonal length of impression)

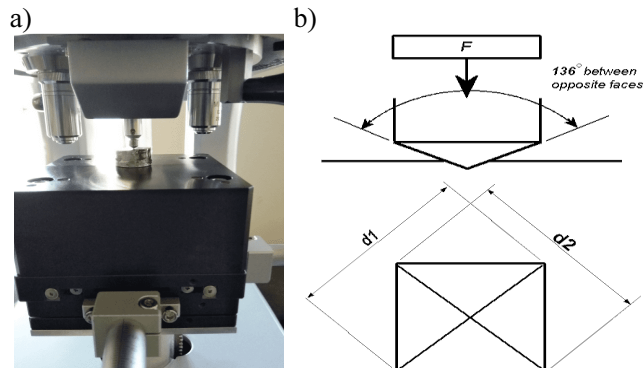


Fig. 6. Vickers hardness tester (a), impression of square pyramid indenter (b)

Wear test

A pin-on-disc apparatus (as shown in Figure 7) was used to investigate the wear characteristics of the Al alloy and its composites at various loads under dry conditions. In this test, the rotational speed of 600 rpm and track radius of 60 mm were kept constant and the normal load was varied from 20 to 40 N in steps of 10 N, the results of which are shown in Figure 13. The specimens were prepared as per ASTM G99 standards as shown in Figure 8. For smooth sliding action between the composite pin and the rotating disc, the sample was polished with emery paper and the disc was cleaned (using an acetone solution and a non-fabric cloth) after each test to prevent the entrapment of wear debris from earlier tests. In this test, the wear rate was measured with electronic sensors and stored on a PC.

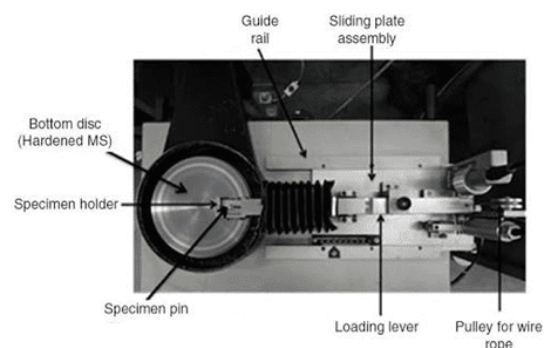


Fig. 7. Pin-on-disc apparatus

SPECIMEN SPECIFICATIONS

Specimens prepared as per the standard are shown in Figure 8.



Fig. 8. Wear test specimens; Pin diameter = 10 mm; Pin length = 30 mm

CORROSION TEST

A corrosion test was carried out (Andhra University) on an ACM Instruments Gill AC 1339 (Fig. 9) according to the ASTM B117 standard in which the specimen was exposed to a 3.5 wt.% NaCl solution for 2 h at the sweep rate of 10 mV/min. The equipment contains a cell with an Ag/AgCl reference electrode, a counter electrode (platinum) and a facility for attaching the working electrode (manufactured specimen).

The working electrodes for the corrosion test were taken from prepared composites having the dimensions 15 mm in diameter and 10 mm in thickness. These specimens were polished with emery papers and after that disc polishing was carried out to obtain a smooth polished surface. The area of the specimen to be exposed to the electrolyte solution was approximately 1 cm². The potential (E_{corr}) and current density (i_{corr}) were determined using the Gill AC and the obtained Tafel plots were saved on the PC.



Fig. 9. ACM Instruments Gill AC 1339

RESULTS AND DISCUSSION

Tensile strength

Figure 10a and b shows that the ultimate tensile strength of the Al6061/5 wt.% SiC composite with 6 wt.% WC is higher compared to the base alloy

Al6061 and other the composites due to the existence of the highest percentage of WC particles and also because of the good bonding strength between the base alloy and the dispersed fine-grained WC particles [5]. A total of 15 samples (3 for each composition) were tested for tensile strength to obtain reliable values on a computerized tensile testing machine INSTRON 8801. The addition of 2 wt.% WC to Al 6061/5 wt.% SiC raises the tensile strength of the composite as shown in Figure 10b. Additionally, increasing the wt.% of the WC particles to the Al 6061/SiC composite further increases the tensile strength as a result of the fact that the reinforcing particles obstruct the dislocation movement in the Al6061 alloy matrix via the dispersion strengthening mechanism and the distance between the particles reduced by increasing the amount of WC will raise the necessary tension for particle dislocation, and enhance the strength of the composite [4]. Similar results were presented by Rajesh [23] in his work, that the strength of the Al6061/WC composite grows up to the addition of 3 wt.% WC but with a further increase in reinforcement, clusters are formed, resulting in the development of internal stresses that obstruct the increase in strength. In the present work, the ultimate tensile strength increased by 19.39% as compared to the base composite.

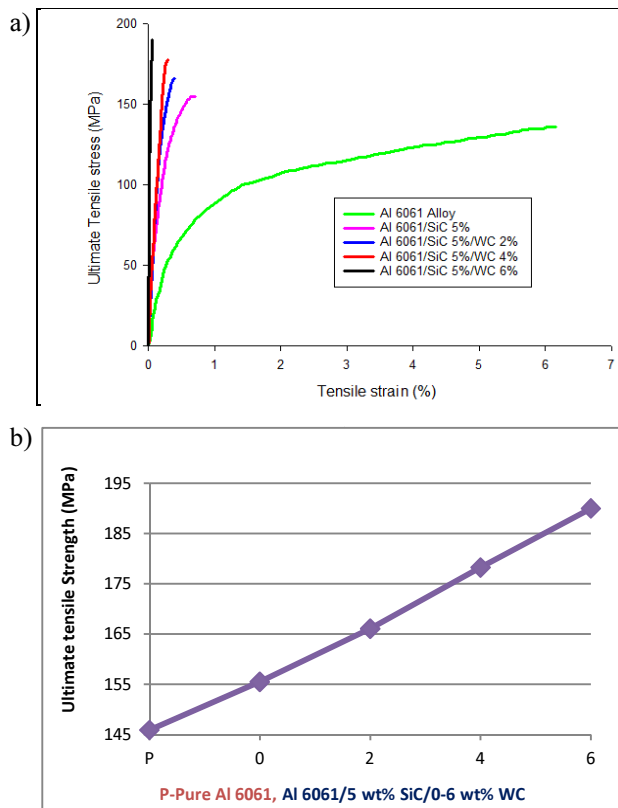


Fig. 10. Ultimate strength vs. tensile strain (a), variation in UTS of different composites (b)

The improvement in the ultimate tensile strength may be a consequence of the different strengthening mechanisms that arose: grain size refinement, homogeneous distribution of the reinforcing particles, good in-

terfacial bonding between the matrix and particles, as well as variance in the thermal expansion coefficient of the base alloy and particles [24]. The large difference in the thermal expansion of the Al alloy and WC leads to increased dislocations close to their interface, which occurs to be an obstacle to the free movement of dislocations [25], and exceptional bonding at the matrix particle interface allows transfer of the tensile load to the WC particulates by interfacial shear stress; as a result, the strength of the composite increases [26]. The finer grain size of the particle shortens the space among the distributed reinforcing particles, restricts the dislocation movement, leading to an rise in the strength of the composite [27]. The modulus of elasticity of the Al6061 alloy is 67.89 GPa and for the composite with 5 wt.% SiC it increased to 83.15 GPa, while the highest value of 89.82 GPa was achieved by the Al6061/5 wt.% SiC composite with 6 wt.% WC. The change in the modulus of elasticity is higher for the Al6061/SiC composite than that of the base alloy but it does not make much difference compared to the composite with WC.

Fracture morphology

Figure 11a reveals that the base alloy Al 6061 totally fractures in a ductile nature and large voids with more dimples are be visible on the fracture surface of the base alloy. Figure 11b shows that in the composite with 5 wt.% SiC the dimples are reduced compared with the base alloy and there the shear lips are larger, indicating a high elongation percentage resulting from the highly ductile nature of the composite with 0 wt.% WC. This composite has a low ultimate strength, but it is higher than the base alloy. In Figure 11c the 2 wt.% WC hybrid composite a further decrease in the size of the shear lips can be observed, which demonstrates the relatively higher ultimate strength. The SEM micrograph in Figure 11d reveals that the composite with 4 wt.% WC still has a smaller lip size, indicating that the fracture mode is in transition from a ductile to a brittle nature. The UTS and hardness values were further increased. In the 6 wt.% WC hybrid composite shown in Figure 11e, the fracture is completely brittle without evidence of shear lips. Due to the higher concentration of WC, the ultimate strength and hardness were highest.

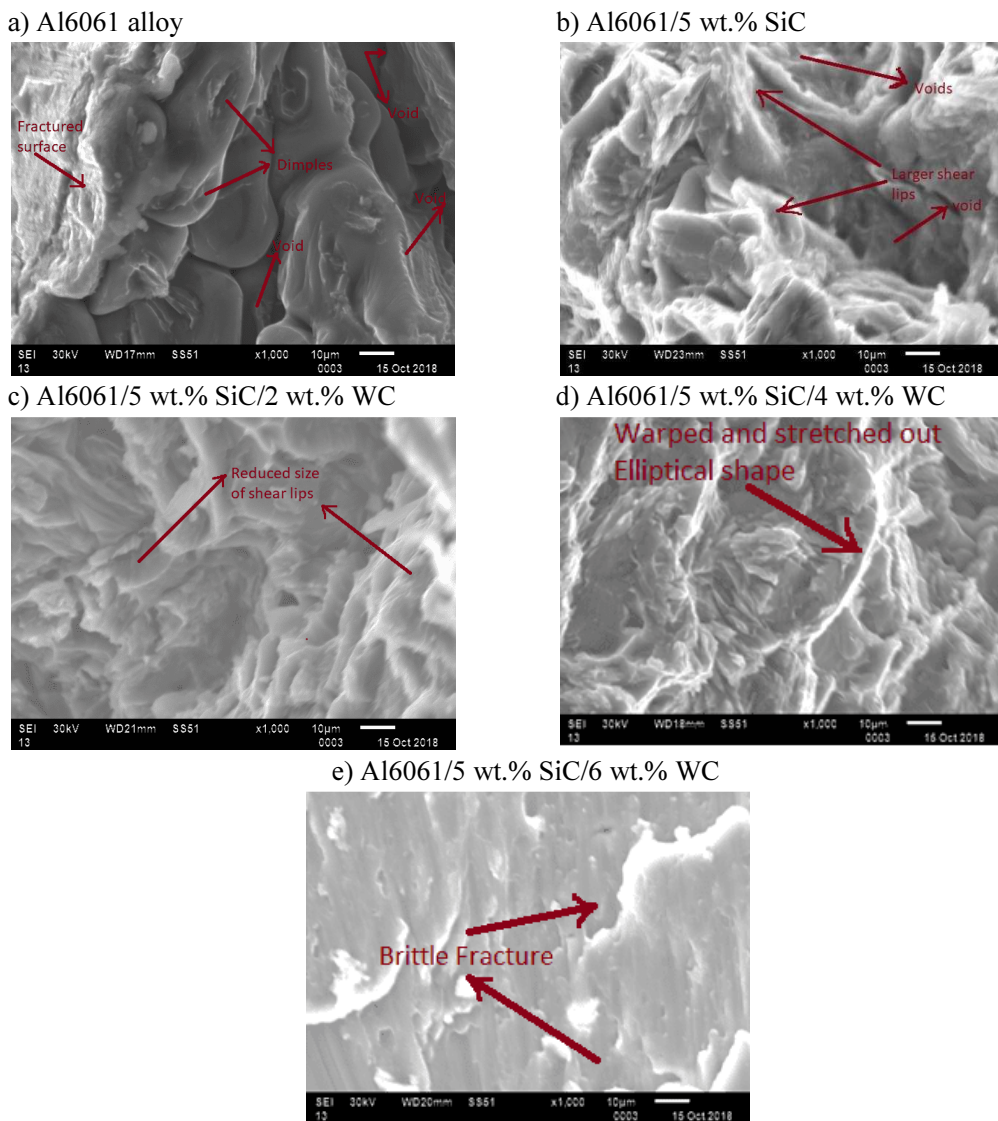


Fig. 11. SEM micrographs of Al6061 and its composites

The fracture morphology of Al6061/SiC/WC hybrid composites reveals that the reinforcing particles clearly visible at the grain boundary cavity in the etched matrix form Mg₂Si with a larger grain size and some undisclosed Al₆ (Fe, Mn) in the base alloy distributed uniformly all over the matrix, enhance the mechanical properties of aluminium hybrid composites [6]. Shankar Subramanian [28] stated that the fractography of a tensile tested specimen shows that the reinforcing particles are distributed uniformly and it is observed that the fracture of the composite containing 6 wt.% WC occurred in a ductile nature because of the fact that the well-bonded particles are highly warped and stretched out into an elliptical shape under the tensile load as shown in Figure 11d, and this shape occurred owing to the formation of particle clustering of fine-grained silicon particles. The fracture morphology of Al 6061 with 5 wt.% SiC and TiB₂ particulates reveals that there is a reduction in the size of voids with the incorporation of reinforcing particles compared to that of the base alloy, and the well-positioned TiB₂ particles inside the dimples confirms that the enhanced bonding between the matrix and reinforcing particles at their interface leads to an increment in the ultimate tensile strength [29]. The fractography of the hybrid aluminium composite shows that the surface crack was both intergranular and transgranular and it was observed that there is a mixed-mode of fracture, particle pull-out regions, and small dimples, which hold high strength before fracture [30]. However, by increasing the wt.% of WC particles, further fragile regions near the Al/WC interfaces were observed, inducing the initiation and propagation of cracks near the matrix-reinforcement interfaces, which leads to quick failure [24].

Hardness

The bar graph displaying the Vickers hardness (HV) of the different samples is shown in Figure 12. It can be observed from Table 4 that the hardness of the reinforced composites is higher than that of the pure Al alloy and the highest hardness of 81.89 HV was found for the Al/5 wt.% SiC composite at the highest percentage of WC and the lowest value for the base alloy of 52.57 HV. The hardness values of the composites are higher than the Al 6061 alloy, as shown in Figure 12, as a consequence of the presence of stronger and stiffer SiC and WC particles [6], restraining the plastic deformation of the matrix during the hardness test and these particles of different sizes make the identical atomic layers in the base alloy less regular [31]. The composite with 5 wt.% SiC combined with WC exhibits greater hardness than that of the base alloy and the highest hardness was found for the composite with 6 wt.% WC, whose density is 5 times more than that of SiC and also sustains the maximum load transferred by the Al6061 matrix [3, 32, 33]. Anish [34] in his paper stated that the composite with 6 wt.% WC possesses the highest hardness and an additional increase in this particulate

results in a reduction in hardness due to particle agglomeration. Swamy et al. [5] and Ajay Ram Krishna et al. [35] reported a different tendency, namely that the hardness value decreases with an addition of WC below 6 wt.% owing to the poor wettability between the reinforcing particle and the Al 6061 alloy. In this study, it was observed that the hardness increased by 24.8% with the addition of WC particles to 6% by weight. The rise in hardness of the Al alloy is a result of the strengthening of the base metal by increasing the volume fraction of WC, which reduces the average grain size of the particle and smaller size reinforcing particles form a greater number of grain boundaries that obstruct the plastic deformation of matrix [24]. Usually, SiC and WC ceramic particles are hard due to the existence of covalent bonds and ionic bonds together and a great amount of energy is needed to break them as a consequence of the presence of ionic bonds [31]. Higher hardness can be obtained for the composite at its highest percentage of reinforcing particles, which leads to improved wear resistance according to Archard's law, but it inversely affects the machinability of the composite. The improved hardness and wear resistance of the composite negatively impact the machinability of the composite owing to the presence of hard ceramic particles. This is due to the fact that during machining of the composite, detached reinforcing particles cause gaps on the surface, leading to greater surface roughness of the composite, and in turn, result in poor machinability of the composite. Nonetheless, better machinability can be attained by the composite with a lower wt.% of reinforcement at a constant speed and feed rate compared to the presence of a higher wt.% of particles [1, 8].

TABLE 4. Vickers hardness of Al 6061 alloy and Al 6061 alloy composites

S. No	% composition	HV
1	Al 6061 alloy	52.57
2	Al 6061/5 wt.% SiC	59.98
3	Al 6061/5 wt.% SiC/2 wt.% WC	72.43
4	Al 6061/5 wt.% SiC/4wt.% WC	76.62
5	Al 6061/5 wt.% SiC/6 wt.% WC	81.89

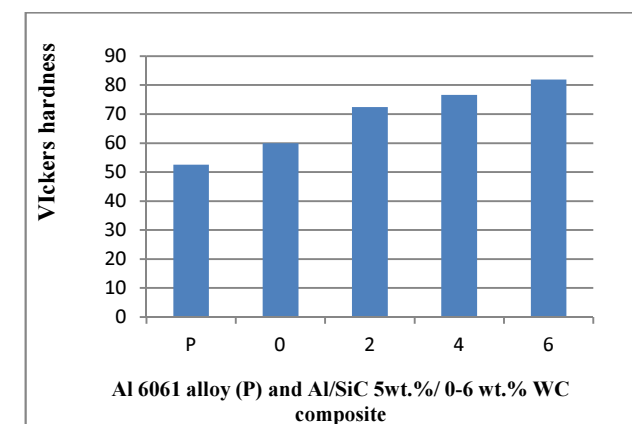


Fig. 12. Different wt.% of composition vs. hardness

Wear analysis

Figure 13 reveals that the hard reinforced SiC and WC particles in the Al 6061 alloy enhance the wear resistance to a great extent. Consequently, it can be reasoned that the filler particulates limit the plastic flow of the alloy, resulting in more uniform wear [35]. From the plot, it is observed that the influence of the WC particles on the wear properties of the composites was great. High wear loss is observed for the base alloy and next for the composite with 5 wt.% SiC and the least for Al 6061/5 wt.% SiC containing 4 wt.% WC particles at the higher load, as shown in Figure 4. Moreover, it can be observed that there is no considerable change in the wear loss for 4 wt.% WC particles at the higher load, probably due to the balance between the hardness and de-bonding of the WC particles. Higher hardness does not mean greater wear resistance or a lower weight loss because the wear rate may be influenced by other factors like toughness and particle distribution. An insufficient amount of the wetting agent may be one of the reasons for the inferior interfacial strength. The increase in wear loss is observed for the Al 6061/5 wt.% SiC/6 wt.% WC at all the loads is due to de-bonding at the interface and the formation of agglomerations [31]. Arivukkarasan [36] reported that the wear resistance of AMCs is enhanced by increasing the WC owing to the fact that the reinforcing particles become obstacles for the plastic flow of the matrix, resulting in more uniform wear. Similar results were observed by Lekatou et al. [37], that the finer size of the hard WC particles will obstruct the dislocation movement as a consequence of the formation of several interphase boundaries and the dispersion of hard particles, along with the presence of a wide range of intermetallic compound particles (Al_5W , Al_{12}W), which leads to great improvement in the wear resistance. The wear rate of hybrid AMCs is influenced primarily by the size and wt.% of reinforcing particles, whereas the load and sliding speed are considered as secondary and tertiary factors. The wear resistance of the composite improved at the presence of the highest wt.% of particles with a finer grain size. It was stated that the accumulation of reinforcing particles prevents dislocation movement and the filler particles form a thin protective layer between the contact surfaces leads to a reduced wear rate [38, 39].

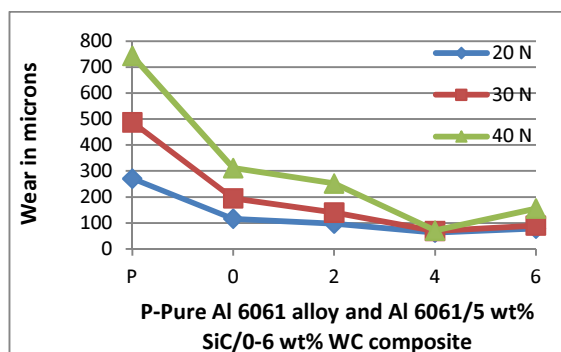


Fig. 13. Wear of Al 6061 hybrid composites

Corrosion behaviour

Figure 14a-b shows the potentiodynamic behaviour of the Al 6061 alloy and the Al 6061/SiC/WC hybrid composites immersed in a 3.5% NaCl solution at room temperature. The E_{corr} , I_{corr} and protection efficiency (μ_p) values obtained for the base alloy and all the composites were tabulated as shown in Table 5. The Tafel extrapolation method was used to study the effect of the SiC and WC particle additions on the cathodic and anodic regions of the specimen. The protection efficiency from the I_{corr} values is calculated using Equation (2)

$$\mu_p \% = \frac{(I_{corr} \text{ of base alloy} - I_{corr} \text{ of composite})}{I_{corr} \text{ of base alloy}} \times 100 \quad (2)$$

The corrosion resistance for the Al 6061/5 wt.% SiC composite was not improved much as the μ_p is only 7.48%, but as WC particles are added to the composition, considerable enhancement is noted. By increasing the wt.% of WC from 2 to 6% at equal intervals of 2%, it was found that the corrosion resistance improves continuously due to the presence of hard ceramic particles, reducing the density of active sites on the composite surface [31]. The highest μ_p of 63.8% was observed for Al/SiC having a 6 wt.% WC content. The passive zone for the base alloy was from a potential value slightly more anodic than -700 mV and it ended where the pitting potential value, E_{pit} , was reached, i.e. -600 mV. The influence of the WC contents on the polarization curves for the different Al6061/SiC/WC hybrid composites is given in Figure 5a-b.

TABLE 5. E_{corr} values of Al 6061 alloy and its composites

S. No	Sample	E_{corr} [mV]	I_{corr} [mA/cm ²]	Protection efficiency [%]
1	Al6061 alloy	-768.62	0.468	—
2	Al6061/5 wt.% SiC	-669.95	0.433	7.48
3	Al6061/5 wt.% SiC/2 wt.% WC	-644.9	0.269	42.5
4	Al6061/5 wt.% SiC/4 wt.% WC	-628.29	0.222	52.5
5	Al6061/5 wt.% SiC/6 wt.% WC	-623.25	0.169	63.8

The polarization curves of Al 6061 and the Al 6061/5 wt.% SiC composites with 0, 2, 4, and 6 wt.% WC are shown in Figure 14a-b. It can be observed from the plots that the potential (E_{corr}) values of the composites are higher than that of the base alloy; this may be due to the existence of intermetallic compounds that act as the cathodic on the base alloy, which caused the pitting corrosion to increase [40]. Moreover, the accumulation of hard WC particulates in the base alloy can reduce the corrosion rate owing to the even dispersion of reinforced particulates [36]. The WC reinforced composites exhibit higher cathodic current densities compared with the Al/SiC composite resulting from the existence of Al_{12}W , Al_5W and $\text{Al}_3(\text{SiC},\text{W})$ intermetallic

compounds. Coarse particles with intermetallic compounds have a large enough surface area that can sustain the cathodic reactions [37]. The E_{corr} values of Al 6061 and its composites obtained by the corrosion test (Table 3) reveal that the composite with 6 wt.% WC exhibits greater corrosion resistance than other composites.

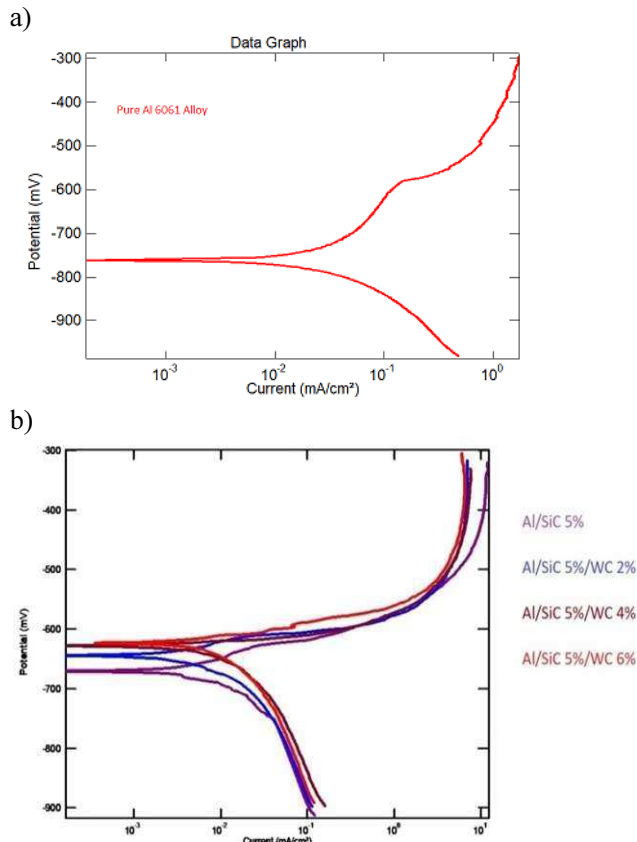


Fig. 14. Polarization curves for pure Al 6061 alloy and its composites (components in wt.%)

Morphology of corroded surface

From Figure 15 a-e, it can be observed that the Al6061 alloy endured higher corrosion than that of its composites as the reinforcing particles act as cathodic sites with galvanic action [36]. The reinforcing hard ceramic particles fill the voids, holes and defects on the surface of composite so that metal dissolution was slowed down [31]. Figure 15a reveals the results of the corrosion test on the Al 6061 alloy, indicating that some deep corroded areas are identified due to the passage of electrolytic ions. Even though the corrosion resistance of the composite with 5 wt.% SiC is higher than that of the matrix, it is observed that there are pitting formations on the surface of the Al/SiC composite with 0 wt.% WC as shown in Figure 15b. Moreover, increasing the wt.% of the WC particles gradually reduces the pit density in comparison to that of the Al6061 alloy, as shown in Figure 15c-e. The localized dissolution of Al (anodic) leads to the formation of small pits as a consequence of the difference in the electrochemical potential between aluminium and iron aluminide or Al and Al-Fe-Si, whereas differential aeration cells were made between the pit walls and the bottom area of a pit as the pits get deeper. At the Al-Fe intermetallic boundaries, this pitting was advanced to intergranular corrosion [37].

SEM/EDS analysis

The microstructure of the Al 6061/SiC/WC composites was studied by scanning electron microscopy (SEM) along with energy dispersive spectroscopy (EDS) to identify the elemental composition of the sample with 5 wt.% SiC and 6 wt.% WC. Figure 16a-b shows the distribution of WC on the Al6061/SiC surface and the elemental content of composite.

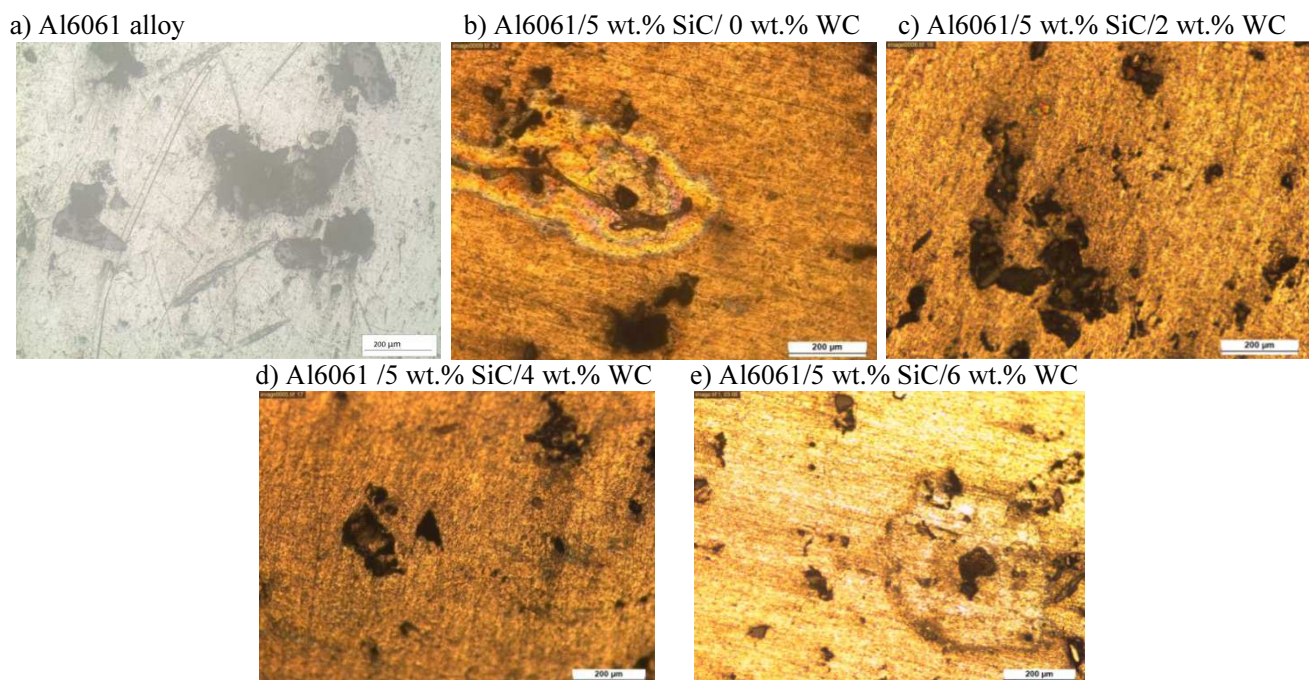


Fig. 15. Microstructures of corroded surfaces of Al 6061 and Al 6061 hybrid composites

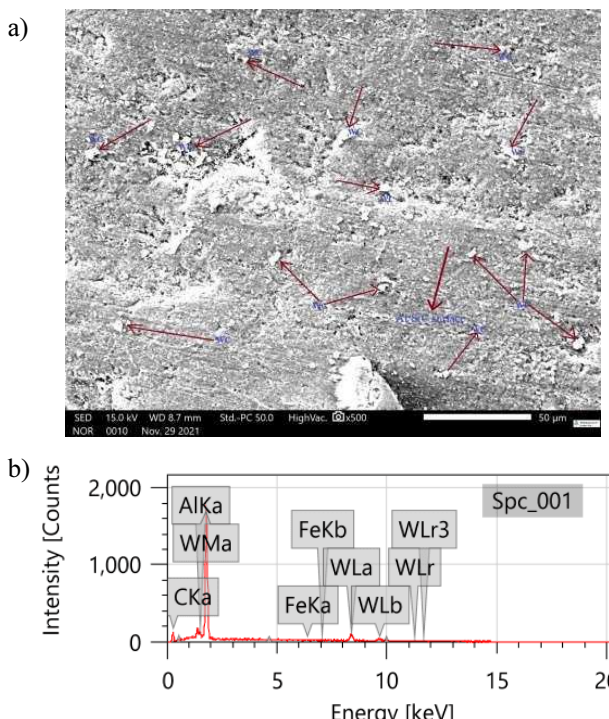


Fig. 16. a) WC particle distribution on Al/SiC surface; b) EDS elemental composition of composite

In Figure 16a, uniform distribution of the WC particles over the Al/SiC surface for 6 wt.% WC reinforcement can be observed. The EDS results in Figure 16b demonstrate that thanks to the addition of reinforcement, there was an increase in the Si content that reacts with oxygen and forms SiO_2 , which improves mechanical properties like strength and hardness [41]. The energy dispersive spectrum shows the existence of aluminium (Al), carbon (C), silicon (Si) and tungsten (W), in the sample. It is observed that at the highest weight percentage of reinforcement, the C and Si content in the composite reaches the peak level, resulting in comprehensive dispersion of the particles in the base matrix [31].

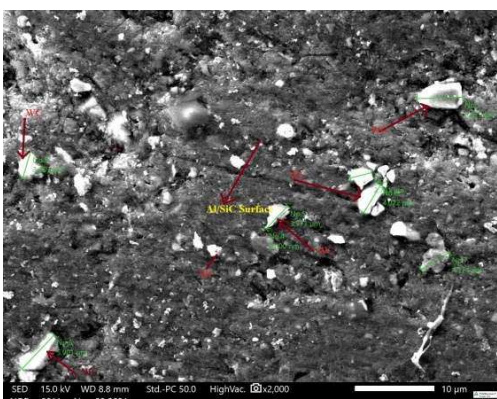


Fig. 17. Grain size of WC particles (3–5 μm)

The SEM micrograph in Figure 17 reveals that the average grain size of the distributed WC particles is 3–5 μm over the surface of the Al/SiC composite. Mechan-

ical properties like strength and hardness are improved by increasing the wt.% of the WC reinforcement and the smaller the grain size of the particles resulted in a rise in displacement compactness caused by the reinforcing hard ceramic particles and a greater interfacial area between the two different phases of matrix and particles [27, 37, 42]. A. Lekatou et al. [37] stated that Al reinforced with WC forms two different tungsten aluminides at different temperatures, i.e. at the melting temperature (830°C) Al_5W and during cooling (697°C) Al_{12}W intermetallic compounds improve the hardness and wear resistance due to the presence of highly dense aluminide and carbide particles.

CONCLUSIONS

The composites were produced by the stir casting process using aluminium 6061/5 wt.% SiC as the base composite and WC as the reinforcement with varying wt.% - 0, 2, 4, and 6.

The tensile test results reveal that the strength of the composites was improved as the wt.% of WC increases compared to that of the base composite, and the highest strength was attained by the composite with 6 wt.% WC particles as a consequence of strong bonding between the matrix and reinforcing particles at their interface.

The hardness of the composites increased with the addition of WC in comparison to that of the base composite and was the highest in the 6 wt.% WC composite. It was inferred that as a result of the presence of WC with SiC particulates in the base alloy, the plastic deformation of the composite is constrained and the hardness of the composites is greater at the periphery of the particles distributed in the base alloy because of increased strain energy [43].

The wear rate of the composites with 0 wt.% WC rose by increasing the normal load and at 2 wt.% WC, it reduces to a great extent at higher loads. It is observed that at 4 wt.% WC the wear loss is less at lower loads but there was no change at higher loads, probably as a consequence of the balance between hardness and debonding of WC particles, and at 6 wt.% WC the wear loss increased somewhat, perhaps owing to de-bonding at interface and formation of agglomerations. Moreover, there is a chance of causing more friction with a higher load at the contact surfaces, leading to a rise in material wear [6]. The number of voids is reduced because of the presence of WC particles and dislocation pile-up also occurs as the wt.% of filler particles is increased, which results in limitation of the plastic flow of the matrix, leading to a decline in wear loss up to 4 wt.% WC, while a further increase in the wt.% of WC causes more wear loss due to insufficient wettability [35].

The Al 6061 hybrid metal matrix composites displayed a reduced corrosion rate compared to the base composite in 3.5 wt.% NaCl solutions by the gradual wt.% additions of WC with a constant SiC content of 5 wt.%. The corrosion test results reveal that the corro-

sion of the Al 6061 alloy is more than the composite with reinforcement and exceptional corrosion resistance was obtained by the composite containing 6 wt.% WC.

There is evidence from the SEM micrographs (Figs. 16a-17) that the mechanical properties of the composite were improved as a result of the uniform distribution and finer size of the WC particles at their highest wt.%.

Future scope

This work can be further extended by varying the wt.% of SiC particles in the composition of the Al 6061/SiC/WC HMMCs and studying the variation in the mechanical and corrosion properties of the composites.

REFERENCES

- [1] Ozben T., Kilickap E., Çakır O., Investigation of mechanical and machinability properties of SiC particle reinforced Al-MMC, *Journal of Materials Processing Technology* 2008, March, 198, 220-225, DOI: 10.1016/j.jmatprotec.2007.06.082.
- [2] Md. Rahman H., Mamun Al Rashed H.M., Characterization of silicon carbide reinforced aluminium matrix composites, *Procedia Engineering* 2014, 90, 103-109, DOI: 10.1016/j.proeng.2014.11.821.
- [3] Ravikumar K., Kiran K., Sreebalaji V.S., Characterization of mechanical properties of aluminium/tungsten carbide composites, *Journal of Measurement* 2017, May, 102, 142-149, DOI: 10.1016/j.measurement.2017.01.045.
- [4] Arivukkarasan S., Dhanalakshmi V., Stalin B., Ravichandran M., Mechanical and tribological behaviour of tungsten carbide reinforced aluminium LM4 matrix composites, *Particulate Science and Technology* 2017, May, 36, 967-973, DOI: 10.1080/02726351.2017.1331285.
- [5] Swamy A.R.K., Ramesha A., Prakash J.N., Veeresh Kumar G.B., Mechanical and tribological properties of As-cast Al6061-tungsten carbide metal matrix composites *Journal of Material Science Research India* 2010, April, 7, 355-368, DOI: 10.13005/msri/070205.
- [6] Fenghong C., Chang Ch., Zhenyu W., Muthuramalingam T., Anbuczezhiyan G., Effects of silicon carbide and tungsten carbide in aluminium metal matrix composites, *Journal of Silicon* 2019, January, 11, 2625-2632, DOI: 10.1007/s12633-018-0051-6.
- [7] Subramanya Reddy P., Kesavan R., Vijaya Ramnath B., Investigation of mechanical properties of aluminium 6061-silicon carbide, boron carbide metal matrix composite, Springer Science Business Media, Dordrecht, 2017, January, 10, 495-502, DOI: 10.1007/s12633-016-9479-8.
- [8] James S.J., Venkatesan K., Kuppan P., Ramanujam R., Hybrid aluminium metal matrix composite reinforced with SiC and TiB₂, *Procedia Engineering* 2014, 97, 1018-1026, DOI: 10.1016/j.proeng.2014.12.379.
- [9] Bodunrin M.O., Alaneme K.K., Chown L.H., Aluminium matrix hybrid composites: a review of reinforcement philosophies: mechanical, corrosion and tribological characteristics, *Journal of Materials Research and Technology* 2015, October-December, 14, 434-445, DOI: 10.1016/j.jmrt.2015.05.003.
- [10] Alaneme K.K., Ademilua B.O., Bodunrin M.O., Mechanical properties and corrosion behaviour of aluminium hybrid composites reinforced with silicon carbide and bamboo leaf ash, *Tribology in Industry* 2013, March, 35, 25-35, https://www.researchgate.net/publication/279896312_Mechanical_Properties_and_Corrosion_Behaviour_of_Aluminium_Hybrid_Composites_Reinforced_with_Silicon_Carbide_and_Bamboo_Leaf_Ash.
- [11] Alaneme K.K., Sanusi K.O., Microstructural characteristics, mechanical and wear behaviour of aluminium matrix hybrid composites reinforced with alumina, rice husk ash, and graphite, *International Journal of Engineering Science and Technology* 2015, September, 18, 416-422, DOI: 10.1016/j.jestch.2015.02.003.
- [12] Kok M., Production and mechanical properties of Al₂O₃ particle-reinforced 2024 aluminium alloy composites, *Journal of Materials Processing Technology* 2005, April, 161, 381-387, DOI: 10.1016/j.jmatprotec.2004.07.068.
- [13] Pitchayyapillai G., Seenikannan P., Raja K., Chandrasekaran K., Al6061 hybrid metal matrix composite reinforced with alumina and molybdenum disulphide, *Advances in Materials Science and Engineering* 2016, Article ID 6127624, 2016, November, 1-9, DOI: 10.1155/2016/6127624.
- [14] Hima Gireesh Ch., Durga Prasad K.G., Ramji K., Experimental investigation on mechanical properties of an Al6061 hybrid metal matrix composite, *Journal of Composites Science* 2018, August, 49, 2, 1-10, DOI: 10.3390/jcs2030049.
- [15] Kountouras D.T., Stergioudi F., Tsouknidas A., Vogiatzis C.A., Skolianos S.M., Properties of high volume fraction fly ash composites produced by infiltration process, *Journal of Materials Engineering and Performance* 2015, September, 24, 3315-3322, DOI: 10.1007/s11665-015-1612-0.
- [16] Bienia J., Walczak M., Surowska B., Sobczak J., Microstructure and corrosion behavior of aluminum fly ash composites, *Journal of Optoelectron Advanced Materials* 2003, June, 5, 493-502, https://www.researchgate.net/publication/237802225_Microstructure_And_Corrosion_Behaviour_Of_Aluminum_Fly_Ash_Composites.
- [17] Zhiqiang S., Di Z., Li G., Evaluation of dry sliding wear behaviour of silicon particles reinforced aluminium matrix composites, *Materials and Design* 2005, August, 26, 454-458, DOI: 10.1016/j.matdes.2004.07.026.
- [18] Gikunoo E., Omotoso O., Oguocha I.N.A., Effect of fly ash particles on the mechanical properties of an aluminium casting alloy A535, *Material Science and Technology* 2005, July, 21, 143-152, DOI: 10.1179/174328405X18601.
- [19] Vamsi Krishna M., Xavior A.M., An investigation on the mechanical properties of hybrid metal matrix composites, *Procedia Engineering* 2014, 97, 918-924, DOI: 10.1016/j.proeng.2014.12.367.
- [20] Balasivanandha Prabu S., Karunamoorthy L., Kathiresan S., Mohan B., Influence of stirring speed and stirring time on the distribution of particles in cast metal matrix composite, *Journal of Materials Processing Technology* 2006, January, 171, 268-273, DOI: 10.1016/j.jmatprotec.2005.06.071.
- [21] Hima Gireesh Ch., Durga Prasad K.G., Ramji K., Vinay P.V., Mechanical characterization of aluminium metal matrix composite reinforced with aloe vera powder, *Materials Today: Proceedings* 2018, 5, 3289-3297, DOI: 10.1016/j.matpr.2017.11.571.
- [22] Bansal S., Saini J.S., Mechanical and wear properties of SiC/graphite reinforced Al359 alloy-based metal matrix composite, *Defence Science Journal* 2015, July, 65, 330-338, DOI: 10.14429/dsj.65.8676.
- [23] Rajesh D., Anand P., Lenin N., Bupesh Raja V.K., Palanikumar K., Balaji V., Investigations on the mechanical properties of tungsten carbide reinforced aluminium metal matrix composites by stir casting, *Materials Today: Proceedings* 2021, January, 46, 2, 3618-3620, DOI: 10.1016/j.matpr.2021.01.634.

- [24] Huang G., Hou W., Shen Y., Evaluation of the microstructure and mechanical properties of WC particle reinforced aluminium matrix composites fabricated by friction stir processing, *Materials Characterization* 2018, April, 138, 26-37, DOI: 10.1016/j.matchar.2018.01.053.
- [25] Dinaharan I., Nelson R., Vijay S.J. et al., Microstructure and wear characterization of aluminium matrix composites reinforced with industrial waste fly ash particulates synthesized by friction stir processing, *Materials Characterization* 2016, August, 118, 149-158, DOI: 10.1016/j.matchar.2016.05.017.
- [26] Yadav D., Bauri R., Processing, microstructure and mechanical properties of nickel particles embedded aluminium matrix composite. *Materials Science and Engineering A* 2010, October, 528, 3, 1326-1333, DOI: 10.1016/j.msea.2010.10.035.
- [27] Ashok N., Shanmugasundaram P., Effect of particles size on the mechanical properties of SiC-reinforced aluminum 8011 composites, *Materiali In Tehnologije/Materials and Technology* 2016, November, 51, 667-672, DOI: 10.17222/mit.2016.252.
- [28] Subramanian S., Arunachalam B., Nallasivam K., Pramanik A., Investigations on tribomechanical behaviour of Al-Si10-Mg/sugarcane bagasse ash/SiC hybrid composites, *China Foundry* 2019, July, 16, 277-284, DOI: 10.1007/s41230-019-8176-9.
- [29] Justin Maria Hillary J., Ramamoorthi R., Dixon Jim Joseph J., Samson Jerold Samuel C., A study on microstructural effect and mechanical behaviour of Al6061-5%SiC-TiB₂ particulates reinforced hybrid metal matrix composites, *Journal of Composite Materials* 2019, December, 54, 1-11, DOI: 10.1177%2F0021998319894666.
- [30] Niranjan D.B., Shiva Shankar G.S., Shankar L.B., Study on fracture behaviour of hybrid aluminium composite, *Materials Science and Engineering* 2018, January, 144 1-6, DOI: 10.1051/matecconf/201814402012.
- [31] Bandil K., Vashisth H., Kumar S., Verma L., Jamwal A., Kumar D., Singh N., Kumar Sadashivuni K., Gupta P., Microstructural, mechanical and corrosion behaviour of Al-Si alloy reinforced with SiC metal matrix composite, *Journal of Composite Materials* 2019, June, 53, 1-9, DOI: 10.1177%2F0021998319856679.
- [32] Velmurugan C., Investigations on the effect of tungsten carbide particles on the hardness and wear properties of aluminium composite materials, *AIP Conference Proceedings* 2020, November, 2270, 1, 030007-1-030007-7, DOI: 10.1063/5.0020308.
- [33] Ebenezer Jacob Dhas D.S., Velmurugan C., Leo Dev Wins K., BoopathiRaja K.P., Effect of tungsten carbide, silicon carbide and graphite particulates on the mechanical and microstructural characteristics of AA 5052 hybrid composites, *Ceramics International* 2019, January, 45, 1, 614-621, DOI: 10.1016/j.ceramint.2018.09.216.
- [34] Anish A., Ananth Kumar M., Characterization of an aluminium matrix reinforced with tungsten carbide and molybdenum disulphide hybrid composite, *IOP Conf. Series: Materials Science and Engineering*, 2018, March, 402, 1-9, DOI: 10.1088/1757-899X/402/1/012006.
- [35] Ajay Ram Krishna, Arun A., Unnikrishnan D., Karthik V. Shankar, An investigation on the mechanical and tribological properties of alloy A356 on the addition of WC, *Materiastoday: Proceedings* 2018, 5, 12349-12355, DOI: 10.1016/j.matpr.2018.02.213.
- [36] Sambathkumar M., Navaneethakrishnan P., Ponappa K., Sasikumar K.S.K., Mechanical and corrosion behavior of Al7075 (Hybrid) metal matrix composites by two-step stir casting process, *Latin America Journal of Solids and Structures* 2017, February, 14, 243-255, DOI: 10.1590/1679-78253132.
- [37] Lekatou A., Karantzalis A.E., Evangelou A., Gousia V., Kaptay G., Gács Z., Baumli P., Simon A., Aluminium reinforced by WC and TiC nanoparticles (ex-situ) and aluminate particles (in-situ): Microstructure, wear and corrosion behaviour, *Materials and Design* 2015, January, 65, 1121-1135, DOI: 10.1016/j.matdes.2014.08.040.
- [38] Idusuyi N., Olayinka J.I., Dry sliding wear characteristics of aluminium metal matrix composites: a brief overview, *Journal of Materials Research and Technology* 2019, May-June, 8, 3338-3346, DOI: 10.1016/j.jmrt.2019.04.017.
- [39] Gargatte S., Upadhye R.R., Dandagi V.S., Desai S.R., Waghamode B.S., Preparation & characterization of Al-5083 alloy composites, *Journal of Minerals and Materials Characterization and Engineering* 2013, January, 1, 8-14, DOI: 10.4236/jmmce.2013.11002.
- [40] Saravanan S., Senthilkumar P., Ravichandran M., Veeramani Anandakrishnan, Mechanical, electrical, and corrosion behaviour of AA6063/TiC composites synthesized via stir casting route, *Springer* 2017, February, 32, 606-614, DOI: 10.1557/jmr.2016.503.
- [41] Olusesi O.S., Udoye N.E., Development and characterization of AA6061 aluminium alloy /clay and rice husk ash composite, *Manufacturing Letters* 2021, June, 29, 34-41, DOI: 10.1016/j.mfglet.2021.05.006.
- [42] Bhushan R.K., Effect of SiC particle size and weight % on mechanical properties of AA7075/SiC composite, *Advanced Composites and Hybrid Materials* 2020, September, 4, 1-12, DOI: 10.1007/s42114-020-00175-z.
- [43] Gopal Krishna U.B., Ranganatha P., Auradi V., Mahendra Kumar S., Vasudeva B., Microstructural evolution in WC-Co cermet reinforced – Al7075 metal matrix composites by stir casting, *Materials Science and Engineering* 2016, 149, 1-8, DOI: 10.1088/1757-899X/149/1/012090.